Journal of the European Ceramic Society 22 (2002) 463–470

www.elsevier.com/locate/jeurceramsoc

A new approach to anorthite porcelain bodies using nonplastic raw materials

Weon-Pil Tai[a,*], Kunio Kimura[b], Kazuhiko Jinnai[c]

[a]*Institute of Advanced Materials, Inha University, Yonghyun-Dong, Nam-ku, Inchon 402-751, South Korea*
[b]*Inorganic Materials Department, Kyushu National Industrial Research Institute, Tosu, Saga 841-0052, Japan*
[c]*Advanced Science and Technology Center for Cooperative Research, Kyushu University, Kasuga, Fukuoka 810-8580, Japan*

Received 10 June 2000; received in revised form 26 March 2001; accepted 28 April 2001

Abstract

New anorthite porcelain bodies using only nonplastic raw materials, such as feldspar, quartz, and aluminous cement, without using a binder were fabricated, and their properties were investigated. The green strength was relatively high due to hardening by the hydration reaction of the aluminous cement with the feldspar in a moist atmosphere. The phases found in the green body were feldspar, $CaAl_2O_4$, $CaAl_4O_7$, α-quartz and a small amount of $CaAl_2Si_2O_8{\cdot}4H_2O$. The phases in the fired body were α-quartz, anorthite, glass and a small amount of α-Al_2O_3; cristobalite formed only at a quartz content of 60 wt.%. Higher flexural strength at a composition containing 30 wt.% feldspar is attributed both to fewer crack origins as a result of appropriate vitrification and to greater residual stress caused by the larger difference in the thermal expansion coefficient between the glass matrix and the quartz and anorthite grains.

Keywords: Porcelains; Anorthite; Phase development; Mechanical properties

1. Introduction

Porcelains are generally fabricated using quartz, feldspar, and clay minerals which act as plastic raw materials. These feldspar–quartz–clay systems are well known as the basis for a porcelain body. The fabrication of a porcelain body using plastic raw materials has been long established.[1–4] Many studies have been performed for the improvement of the mechanical strength of porcelain bodies.[4–6] The strength of a fired body increases by controlling the size of quartz grains to approximately 30 μm. The residual stress in a fired body is one of the main factors to increase the strength, because a strong compressive stress generated in the glassy phase surrounding the quartz grains as a result of the large difference in the thermal expansion coefficient between the glassy phase and the quartz grains, resists crack extension.[7,8] The replacement of quartz by α-alumina[6,9] and an increase of the mullite content[10] strengthen the fired body.

The resources of high-grade plastic raw materials have recently begun to become depleted, especially in Japan, Korea and North America. However, it needs much cost to refine low-grade plastic raw materials. Thus, a new approach to the development of porcelain bodies without using plastic raw materials is necessary. Plastic raw materials are normally required because they provide plasticity for forming, and transform into glass and crystalline phases during firing. In the present study, the plastic raw materials have been replaced by an aluminous cement (calcium aluminate cement). The aluminous cement can increase the green strength by the hydration reaction[11] in moist atmospheres without using any binder or plastic raw materials. It also melts with the feldspar and quartz during the firing process, and the melted glassy phase crystallizes and becomes anorthite ($CaO{\cdot}Al_2O_3{\cdot}2SiO_2$).[12]

The purpose of this study is to try the fabrication of a new anorthite porcelain body that possesses high-strength without using a binder, and which is fabricated using only nonplastic raw materials, such as feldspar, quartz and aluminous cement. The physical and mechanical properties of the resultant porcelain bodies are also investigated.

2. Experimental procedure

2.1. Raw materials

The starting materials were alkali feldspar (Nishinihon kohgyo, Japan) of 20–60 wt.%, silica stone (Ube

* Corresponding author. Tel.: +82-32-860-8229; fax: +82-32-874-3382.
E-mail address: wptai@munhak.inha.ac.kr (W.-P. Tai).

0955-2219/02/$ - see front matter
PII: S0955-2219(01)00317-X

industries, Ltd., Japan) of 20–60 wt.% and aluminous cement (Ube industries, Ltd., Japan) fixed to 20 wt.%. As-received feldspar was milled in a pot mill for 6 h. The average particle sizes of the feldspar, silica stone and aluminous cement used are 5.7, 4.6 and 14.5 μm, respectively. The chemical compositions of the raw materials are shown in Table 1. Silica stone consisted of almost pure quartz, which is hereafter designated as quartz, and the aluminous cement consisted of $CaAl_2O_4$ and $CaAl_4O_7$.

2.2. Sample preparation

The starting powders were mixed with various ratios in a planetary mixer for 40 min. The content of added water was 20 wt.%. Fig. 1 shows the body compositions on a ternary diagram. The symbol of 262 in the text means that the mixing ratio of feldspar, quartz and aluminous cement is 20, 60 and 20 wt.%, respectively. The mixed powders were pressed under a pressure of 10 MPa into bars having approximate dimensions of 3.3×5×40 mm. Hydration time was kept for 6, 12, 24 and 48 h at room temperature in moist atmosphere and then the bars were dried in an oven for 24 h at 50 °C. The firing was performed in an electric furnace for 1 h at 1300 °C. The heating rate was 10 °C/min over the temperature range of 25–1000 °C and 5 °C/min in the temperature range of 1000–1300 °C. The cooling rate was 10 °C/min.

2.3. Measurements and analyses

The bulk density of the green body was calculated using the weight and dimensions, ~3.3×5×40 mm. The bulk density of the fired body was determined by water immersion, based on ASTM C20. For surface observation, the specimens were cut using a diamond cutter and then ground by SiC abrasive paper, followed by polishing with diamond paste (3 and 1 μm) and lapping oil. The polished surface of the porcelain bodies was observed by scanning electron microscopy (SEM, ABT, Japan). The polished surface was also etched by 2% HF solution for 1 h. X-ray diffraction (XRD, Philips, Holland) analyses were conducted using Cu K_α radiation to determine the phases in the green and fired bodies. The samples were milled in an alumina mortar and then milled in a vibration mill for 30 s. XRD analyses were also conducted to determine interplanar spacing in the fired bodies. Linear shrinkage was measured using the length direction before and after the firing. Water absorption was measured based on JIS-R2205. The flexural strengths of ~3×4.5×36 mm specimens were measured by using a three-point bending test(Shimadzu, AGS-5KND, Japan) with a lower span of 30 mm under a crosshead speed of 0.5 mm/min, based on JIS-R1601. The surface condition of the measured samples was as-dried in the green bodies, and that for the fired bodies was as-fired. The number of samples used varied between five and seven.

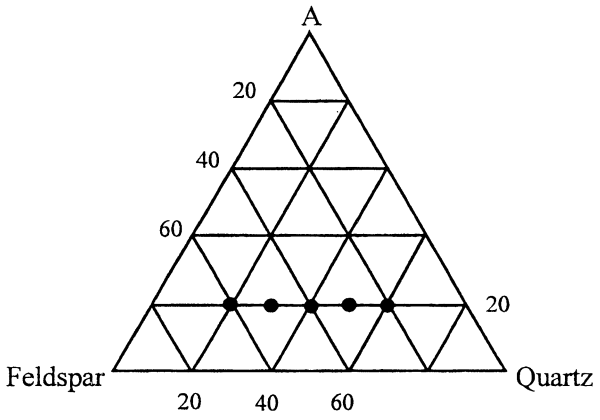

Fig. 1. Ternary diagram showing compositions of the bodies. A, Aluminous cement.

3. Results and discussion

3.1. Effect of hydration time in green bodies

The effect of hydration time on the strength in the green body without using any binders and plastic raw materials was investigated. Fig. 2 shows flexural strength of the green body (green strength) with hydration time in the feldspar–quartz–aluminous cement system (30, 50, 20 wt.%, respectively). The green strength increases with increase of hydration time, slightly up to 12 h, and more markedly up to 24 h. The strength is almost constant at hydration times of 24 to 48 h. The bulk density of the green body also increases with increasing hydration time up to 24 h and then the value remains constant in the range from 24–48 h, as shown in Fig. 3. Fig. 4 shows X-ray diffraction patterns of the 352 green body with hydration time. The phases found in the green body are feldspar, α-quartz, $CaAl_2O_4$, and

Table 1
Chemical compositions of raw materials (wt.%)

	SiO_2	Al_2O_3	Fe_2O_3	TiO_2	CaO	MgO	Na_2O	K_2O	Ig.loss	Total
Feldspar	67.72	17.52	0.17	0.01	0.13	0.10	3.31	10.64	0.39	99.99
Silica stone (quartz)	98.10	1.00	0.20							99.30
Aluminous cement	0.55	70.38	0.14		28.13	0.20				99.40

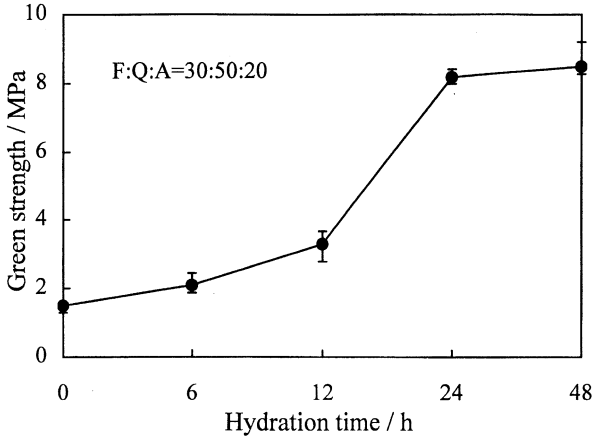

Fig. 2. Variation of green strength of 352 body with hydration time. F, Feldspar; Q, Quartz; A, Aluminous cement. Error bars show the minimum and maximum values observed.

$CaAl_4O_7$. The $CaAl_2O_4$ phase content decreases with increasing hydration time and the phase disappears almost completely at the hydration time of 24 h. However, the $CaAl_4O_7$ phase was stable for a hydration time of 48 h. On the other hand, calcium aluminum silicate hydrate ($CaAl_2Si_2O_8{\cdot}4H_2O$) forms at a hydration time of 24 h. Schneider[13] showed that the reaction of aluminous cement and water produced the metastable hydrates, $CaO{\cdot}Al_2O_3{\cdot}10H_2O$ and $2CaO{\cdot}Al_2O_3{\cdot}8H_2O$ at temperatures of 25 °C or lower, and the stable phases, $3CaO{\cdot}Al_2O_3{\cdot}6H_2O$ and $Al_2O_3{\cdot}3H_2O$ at elevated temperature. In the present study, $CaAl_2Si_2O_8{\cdot}4H_2O$ is formed by the hydration reaction of the aluminous cement with feldspar in the moist atmosphere. The increase of flexural strength in the green body is due to hardening by the hydration reaction, even though the body was formed under low pressure without using any binders and plastic raw materials. The hydration time in all the samples thereafter is set at 24 h in moist atmospheres.

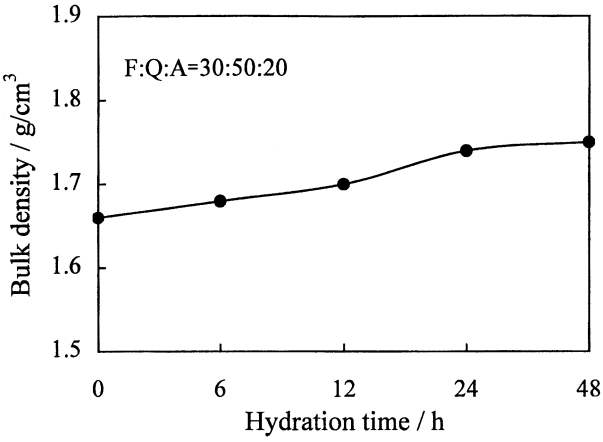

Fig. 3. Bulk density of 352 body with hydration time.

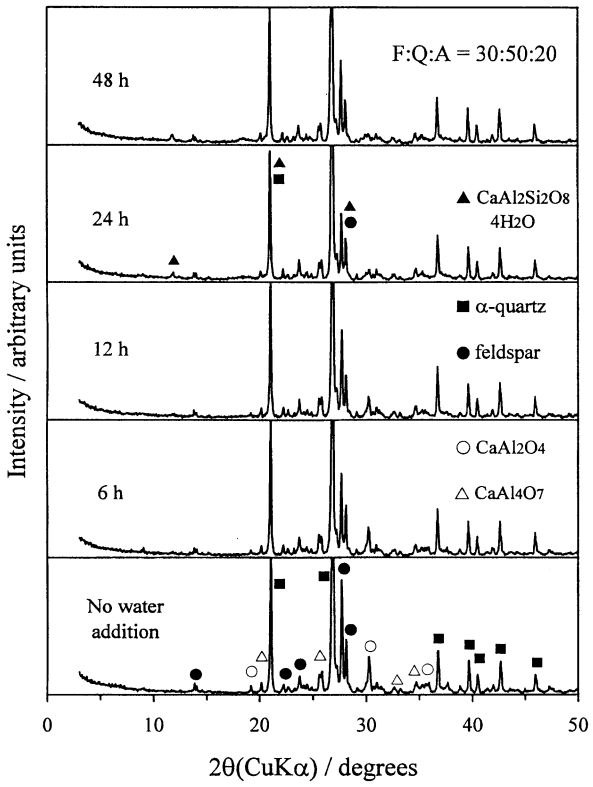

Fig. 4. X-ray diffraction patterns of 352 body with hydration time. F, Feldspar; Q, Quartz; A, Aluminous cement.

3.2. Preparation and properties of green bodies

The green bodies are prepared with various mixture ratios in the feldspar–quartz–aluminous cement system. Fig. 5 shows the change in green strength as a function of composition. The green strength increases slightly with increasing feldspar content, and decreasing quartz content, at a constant aluminous cement content (20 wt.%). The aluminous cement reacts with the feldspar, being a less stable raw material than the quartz in the

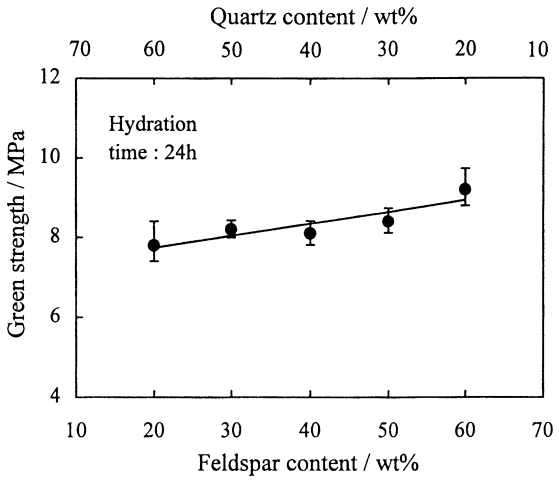

Fig. 5. Variation of green strength as a function of composition in green bodies. Error bars show the minimum and maximum values observed.

moist atmosphere. Addition of 20 wt.% aluminous cement provides a green body of sufficient strength for handling without requiring firing at higher temperature. Fig. 6 shows the bulk density of the green body with various mixture ratios. The bulk density increases slightly with increasing feldspar content.

3.3. Fabrication of porcelain bodies

Fig. 7 shows X-ray diffraction patterns as a function of composition in the fired body heated at 1300 °C for 1 h. The firing temperature is fixed at 1300 °C because the composition of the glaze and underglaze decoration is approximately based on the temperature of 1300 °C. The XRD patterns show that α-quartz, anorthite, glass and a small amount of α-Al_2O_3 are formed at all the batch compositions. However, cristobalite is formed only in the 262 fired body with a larger amount of quartz. Fig. 8 shows the microstructure etched by 2% HF solution in several fired bodies. The large quartz particles remain in the 262 body. In the 622 body, however, a large amount of glass phase is etched away by the HF solution, with pores resulting from over-firing at the same firing temperature of 1300 °C. The 352 body with a highly siliceous glass is less etched by the HF solution, indicating uniform microstructure and appropriate firing. By calculating the integrated intensity of the quartz (100) plane in the 352 raw material mixture and the 352 fired body, the residue of quartz is about 7 wt.% of the total starting quartz content, 50 wt.%. The peak of anorthite increases slightly as shown in Fig. 7. The $CaAl_4O_7$ present in the green body disappeared during the firing process. Anorthite is formed by crystallization from the glassy phase produced from the feldspar, quartz and aluminous cement.[12] The anorthite was also synthesized from kaolin and $CaCO_3$,[14] and SiO_2, $CaCO_3$ and Al_2O_3.[15] In the case of the 30 and 40

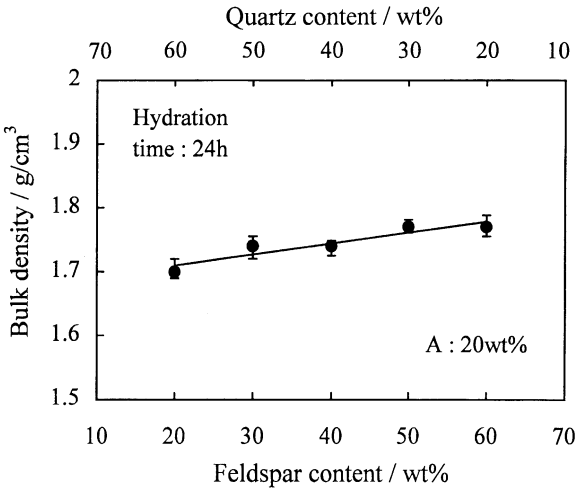

Fig. 6. Bulk density as a function of composition in green bodies. Error bars show the minimum and maximum values observed.

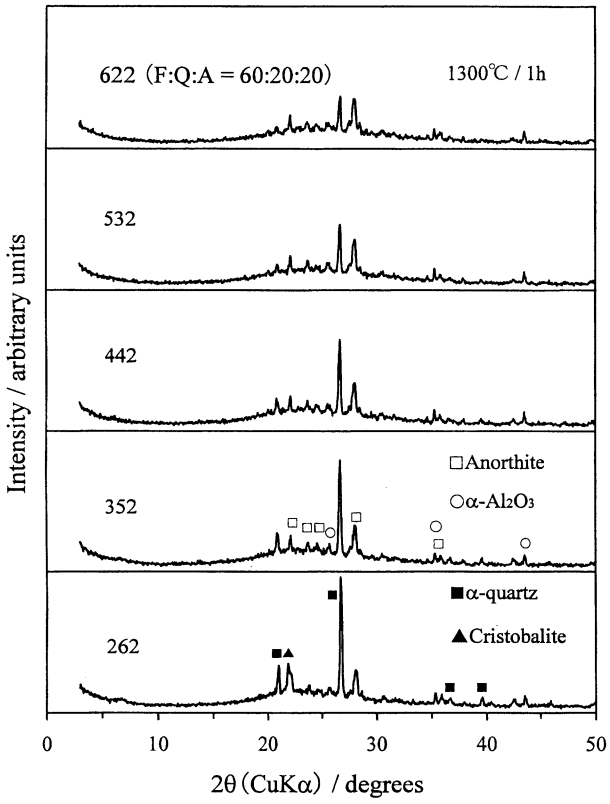

Fig. 7. X-ray diffraction patterns with various compositions in fired bodies. F, Feldspar; Q, Quartz; A, Aluminous cement.

wt.% feldspar contents, the features of the X-ray diffraction patterns are very close to those of a mullite porcelain body,[16] in which the mullite is replaced by anorthite. In general, feldspar melts at around 1100 °C and the melted glass that plays a flux role makes the small quartz particles melt easily. Hamano and Hirayama[7] showed that a small amount of α-cristobalite was formed by the addition of 40 wt.% quartz to pottery stone. Carty and Senapati[17] also reported that cristobalite was crystallized either from the glassy phase or by the direct conversion of quartz. If all the feldspar is melted and 10 wt.% quartz is melted in the respective 262 and 622 mixtures during the firing process, then the SiO_2 content in the glassy phase is higher in the 262 than in the 622 mixtures. The highly siliceous glass is easy to crystallize to cristobalite because it is melted from higher quartz content, i.e., 262 mixture.

3.4. Properties of the porcelain bodies

Fig. 9 shows the bulk density as a function of composition in the fired bodies. The density of the fired body exhibits a maximum value at addition of 30 wt.% feldspar. Generally, the more the alkali-oxides content increases, the lower the viscosity of the glassy phase becomes. In the alumina–feldspar–kaolin system,[9] the addition of feldspar lowers the body vitrification temperature. However, the

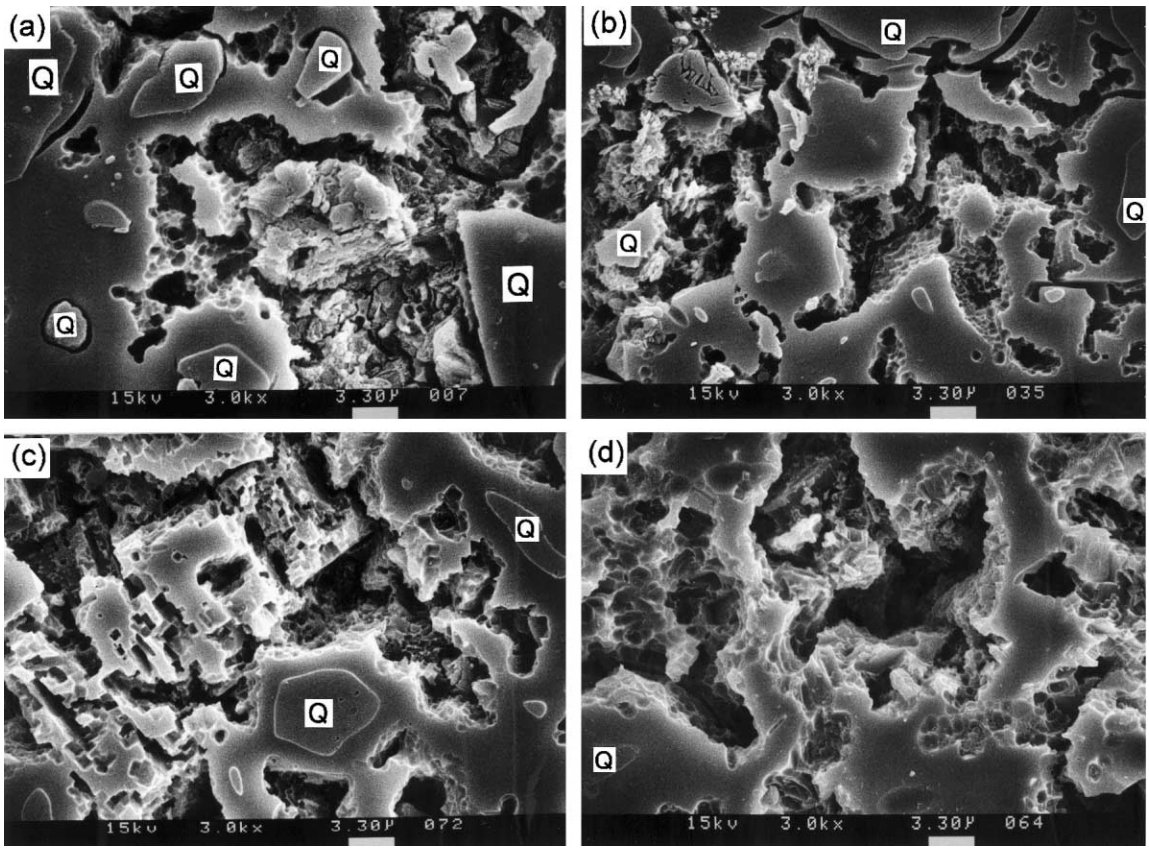

Fig. 8. Microstructure etched by 2% HF solution in (a) 262, (b) 352, (c) 442 and (d) 622 fired bodies.

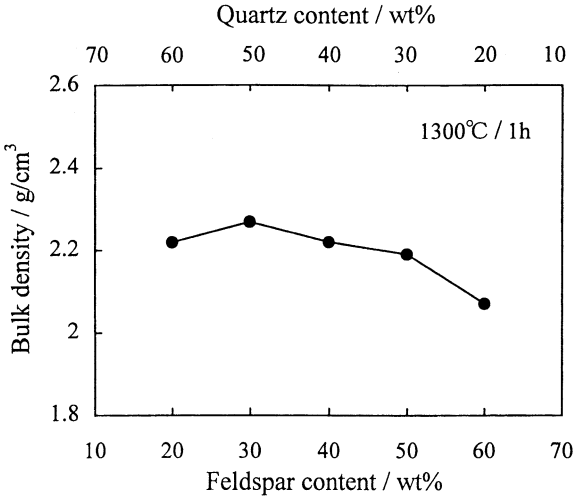

Fig. 9. Bulk density as a function of composition in fired bodies.

lower viscosity at a larger amount of feldspar can induce pores in the body by gas evolution during firing. Fig. 10 shows SEM micrographs of the polished surface as a function of composition in the fired bodies. The addition of larger amounts of feldspar increases the pore size. The decreased density with increasing feldspar content above 40 wt.% feldspar is attributed to the formation of pores in the bodies in the presence of a large amount of low viscosity glass phase during firing. The addition of aluminous cement as a substitute for clays forms anorthite in all the fired bodies. The density of anorthite (2.76 g/cm^3)[18] is low compared with that of mullite (3.16 g/cm^3).[19] In this study, the density is relatively low as 2.07 to 2.27 g/cm^3 due to the formation of anorthite.

Fig. 11 shows the change of flexural strength with various compositions in the fired bodies. Flexural strength attains a maximum value at the addition of 30 wt.% feldspar. In general, quartz particles play a skeleton role in the fired body and, hence, an appropriate quartz amount should be kept for higher strength. Less feldspar addition, i.e. higher quartz content makes the quartz skeleton increase in the glass matrix, as shown in Fig. 7.

Fig. 12 shows the interplanar spacing of the quartz (112) plane in the fired bodies. The interplanar spacing of the quartz standard is shown as a dotted line. The larger interplanar spacing in the fired bodies means that there is a larger residual tensile strain of the quartz grain in the fired body.[20] Hence, a compressive stress is produced on the glassy phase that surrounds the quartz grain in the fired body. The addition of 30 wt.% feldspar (352 body) exhibits a maximum value in the interplanar spacing. The 352 body produces a strong prestress effect[7,8,20] owing to the large difference in the thermal contraction between the glassy phase and the quartz grains during the cooling process.

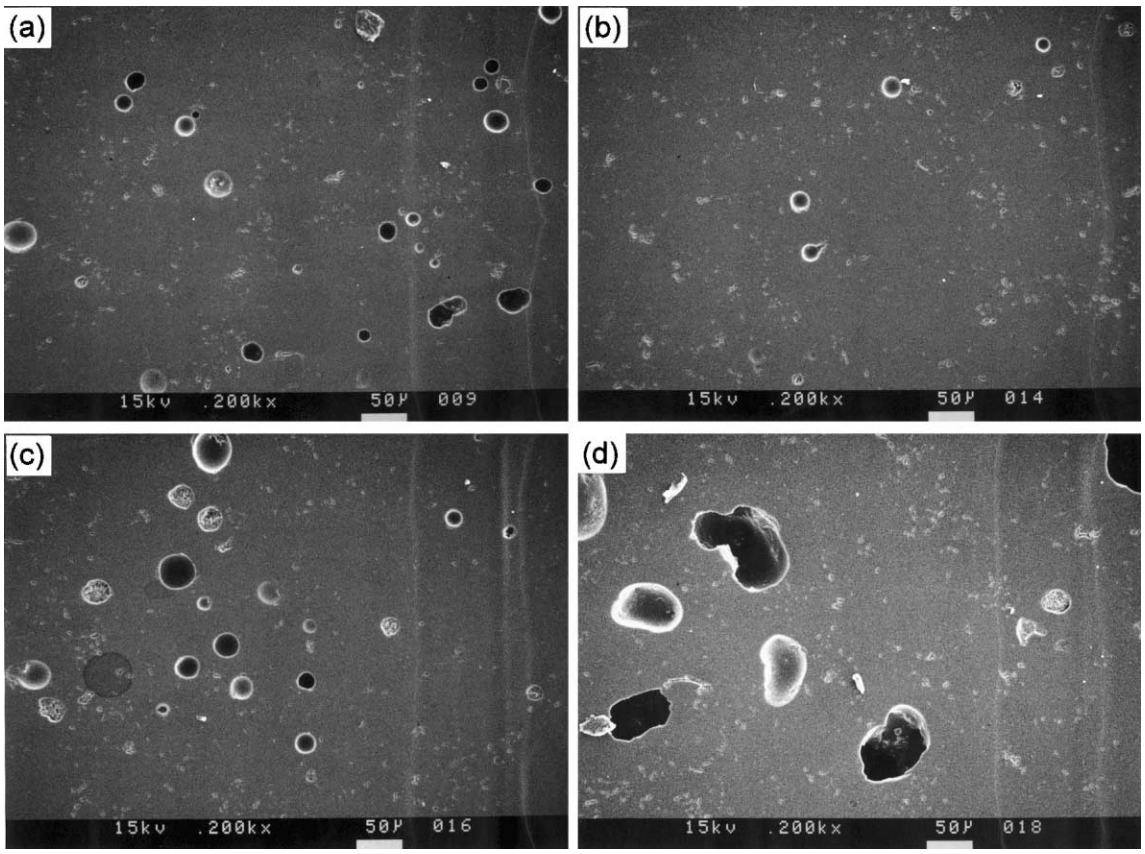

Fig. 10. SEM photographs of polished surface of (a) 262, (b) 352 (c) 442 and (d) 622 fired bodies.

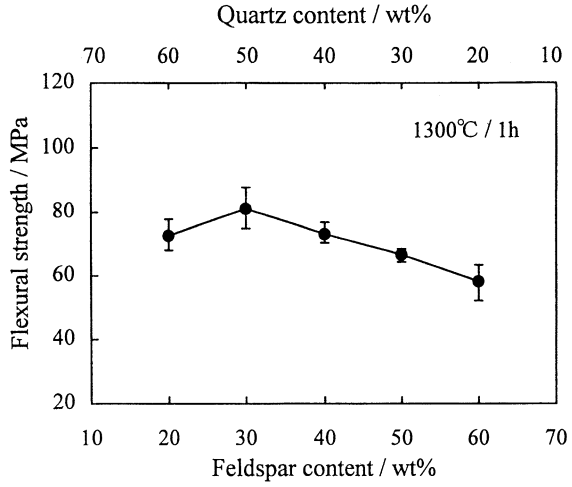

Fig. 11. Variation of flexural strength with various compositions in fired bodies. Error bars show the minimum and maximum values observed.

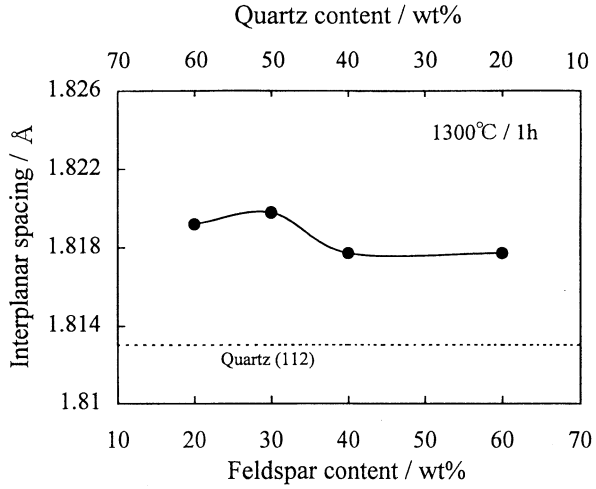

Fig. 12. Interplanar spacing of quartz (112) plane with various compositions in fired bodies. - - - - Quartz (112) standard.

On the other hand, a higher feldspar content lowers the density due to the formation of large pores, as shown in Figs. 9 and 10(d). The large pores can act as fracture origins, with a decrease in the flexural strength.

A small amount of cristobalite is formed in the 262 fired body with higher quartz content. The thermal expansion coefficient of cristobalite is larger than that of quartz. However, Carty and Senapati[17] explained the strength increase in cristobalite porcelain based on the fact that the cristobalite grains were much smaller than the quartz grains. The cristobalite also produced lower strain during the cooling process because the inversion temperature (225–250 °C) of cristobalite is lower than that (573 °C) of quartz. On the other hand, anorthite

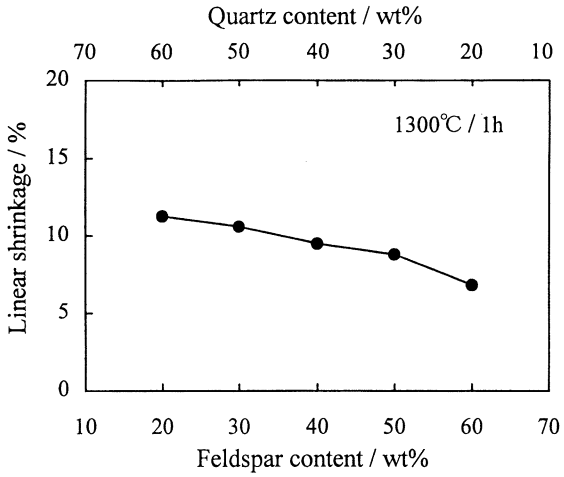

Fig. 13. Linear shrinkage with various compositions in fired bodies.

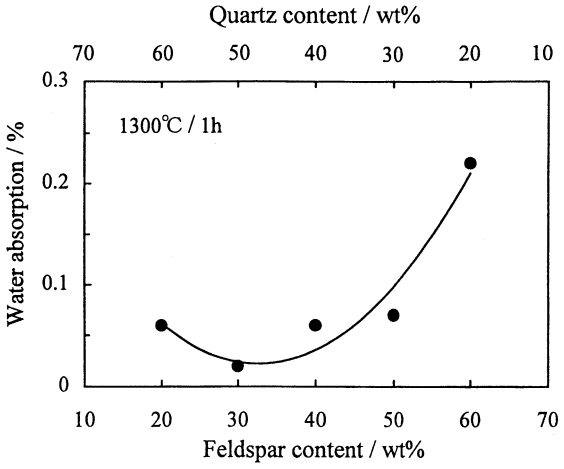

Fig. 14. Water adsorption with various compositions in fired bodies.

crystalline phase in the fired body is formed by the addition of aluminous cement as a substitute for clays. The thermal expansion coefficient of crystalline anorthite is about 4×10^{-6} °C^{-1}.[21] A strong prestress is produced on the glassy phase that surrounds the anorthite grains by the large difference in the thermal expansion coefficient between the glassy phase and the anorthite grains. Higher flexural strength in the 352 body thus is attributed to fewer fracture origins by appropriate vitrification, and to stronger prestress caused by the larger difference in the thermal expansion coefficient between the glass matrix and the quartz and anorthite grains during the cooling process.

Fig. 13 shows linear shrinkage with feldspar content at a constant amount of aluminous cement. The linear shrinkage decreases with increasing feldspar content. The viscosity of glassy phase is lowered by a larger amount of glassy phase with increasing feldspar content and the low viscosity glassy phase induces pores in the body during the firing process. Hence, larger pores form with increasing feldspar content in the fired body, as shown in Fig. 10. The pores of larger size with increasing feldspar content lead to smaller linear shrinkage in the fired body.

Water absorption is measured to investigate the extent of densification in the fired body. Fig. 14 shows the change in water absorption with feldspar content at a constant amount of aluminous cement. Water absorption is small in the ranges 20–50 wt.% feldspar. The water absorption becomes almost 0 at an addition of 30 wt.% feldspar (352 body), which presents a maximum flexural strength as shown in Fig. 11. The very small water absorption indicates that the fired body is well densified even with nonplastic raw materials. However, the water absorption increases with addition of 60 wt.% feldspar (622 body). Such higher feldspar content leads to large pores in the fired body and even at the surface due to a low viscosity glass phase during over-firing, as shown in Fig. 10(d). Increased water absorption in the 622 body is due to the pores formed at the surface caused by over-firing.

4. Conclusions

A new anorthite porcelain body from feldspar–quartz–aluminous cement system without using any binders and plastic raw materials was fabricated at the temperature of 1300 °C and the properties were investigated. The green body is hardened by the hydration reaction of aluminous cement with feldspar in moist atmospheres. The phases formed in the fired body are α-quartz, anorthite, glass and a small amount of α-Al_2O_3; cristobalite only forms with a higher quartz content. The flexural strength of the 352 fired body is increased by the fewer crack origins due to appropriate vitrification and stronger prestress. The addition of aluminous cement as a substitute for clays exhibits a relatively high-green strength and lowers the density due to formation of anorthite in all the fired bodies. A new porcelain body can be produced using nonplastic raw materials without using any binders.

Acknowledgements

This work was supported by the Korea Research Foundation Grant (KRF-99-005-E00033).

References

1. McDowell, S. J. and Vachuska, E. J., The effect of calcined cyanite in porcelain bodies. *J. Am. Ceram. Soc.*, 1927, **10**, 64–74.
2. Austin, C. R., Schofield, H. Z. and Haldy, N. L., Alumina in whiteware. *J. Am. Ceram. Soc.*, 1946, **29**, 341–354.
3. Hamano, K., Wu, Y. H., Nakagawa, Z. and Hasegawa, M., Effect of coarse quartz grains on mechanical strength of porcelain body. *J. Ceram. Soc. Jpn.*, 1991, **99**, 1110–1113.

4. Sugiyama, N., Harada, R. and Ishida, H., Densification process and mechanical strength of feldspathic porcelain body. *J. Ceram. Soc. Jpn.,* 1996, **104**, 312–316.
5. Hamano, K., Nakagawa, Z. and Hasegawa, M., Improvement of mechanical strength of porcelain bodies by fine grinding of raw materials. *J. Ceram. Soc. Jpn.,* 1992, **100**, 1066–1069.
6. Khandelwal, S. K. and Cook, R. L., Effect of alumina additions on crystalline constituents and fired properties of electrical porcelains. *Am. Ceram. Bull.,* 1970, **49**, 522–526.
7. Hamano, K. and Hirayama, M., Effect of quartz addition on mechanical strength of porcelain bodies prepared from pottery stone. *J. Ceram. Soc. Jpn.,* 1994, **102**, 665–669.
8. Mattyasovszky-Zsolnay, L., Mechanical strength of porcelain. *J. Am. Ceram. Soc.,* 1957, **40**, 299–306.
9. Kobayashi, Y., Ohira, O., Ohashi, Y. and Kato, E., Vitrification of whiteware bodies in alumina-feldspar-kaolin system. *J. Ceram. Soc. Jpn.,* 1992, **100**, 743–749.
10. Sane, S. C. and Cook, R. L., Effect of grinding and firing treatment on crystalline and glass content and physical properties of whiteware bodies. *J. Am. Ceram. Soc.,* 1951, **34**, 145–151.
11. Mishima, K., *Seramikku Kogaku Handobukku* (*Ceramic Engineering Handbook*), ed. Ceramic Society of Japan, Gihodo Shuppan, 1989, pp. 1105-07.
12. Levin, E. M., Robbins, C. R. and Mcmurdie, H. F., Fig. 630. In *Phase Diagrams for Ceramists*, ed. M. K. Reser. American Ceramic Society, Columbus, OH, 1964.
13. Schneider, S. J., Effect of heat-treatment on the constitution and mechanical properties of some hydrated aluminous cement. *J. Am. Ceram. Soc.,* 1959, **42**, 184–193.
14. Kobayashi, Y. and Kato, E., Low-temperature fabrication of anorthite ceramics. *J. Am. Ceram. Soc.,* 1994, **77**, 833–834.
15. O, Y. T., Yoshihara, K., Takebe, H. and Morinaga, K., Phase transformations of alkaline-earth aluminosilicate glasses during isothermal heat treatment. *J. Ceram. Soc. Jpn.,* 1997, **105**, 1109–1114.
16. Katsuki, H., A point of contact with the Conventional Porcelain and New Ceramics. *New Ceramics*, 1990, **3**, 1–7 (in Japanese).
17. Carty, W. M. and Senapati, U., Porcelain-raw materials, processing, phase evolution, and mechanical behavior. *J. Am. Ceram. Soc.,* 1998, **81**, 3–20.
18. Cole, W. F., Sorum, H. and Taylor, W. H., The structure of plagioclase feldspars I. *Acta Crystallogr.,* 1951, **4**, 20–29.
19. CRC Handbook of Chemistry and Physics, 74th edn., ed. D.R. Lide, H.P.R. Frederikse. Boca Raton, FL, 1993, pp. 44–37.
20. Hamano, K., Wu, Y. H., Nakagawa, Z. and Hasegawa, M., Effect of grain size of quartz on mechanical strength of porcelain body. *J. Ceram. Soc. Jpn.,* 1991, **99**, 153–157.
21. Ryu, B. and Yasui, I., Sintering and crystallization behaviour of a glass powder and block with a composition of anorthite and the microstructure dependence of its thermal expansion. *J. Mater. Sci.,* 1994, **29**, 3323–3328.